

## FREQUENCY RESPONSES OF NOISE FIGURE AND INPUT MATCHING FOR LOW-NOISE AMPLIFIER DESIGN

<sup>1</sup>JIAN-YU HSIEH, <sup>2</sup>TAO WANG, <sup>3</sup>HUNG-WEI CHIU, <sup>4</sup>YO-SHENG LIN, <sup>5</sup>SHEY-SHI LU, <sup>6</sup>KUEI-YU LIN

<sup>1,6</sup>National Ilan University, Yilan, Taiwan, <sup>3</sup>National Taipei University of Technology, Taipei, Taiwan

<sup>4</sup>National Chi Nan University, Nantou, Taiwan, <sup>2,5</sup>National Taiwan University, Taipei, Taiwan

E-mail: <sup>1</sup>jyhsieh@niu.edu.tw, <sup>2</sup>tw@mail.cgu.edu.tw, <sup>3</sup>hwchiu@ntut.edu.tw, <sup>4</sup>stephenlin@ncnu.edu.tw, <sup>5</sup>sslu@ntu.edu.tw, <sup>6</sup>b0142036@ms.niu.edu.tw

**Abstract-** A method for optimizing a low-noise amplifier (LNA) with understanding Frequency responses of its noise figure (NF) and input matching characteristics is introduced. By determining the quality factors (Q-factors) of the NF ( $Q_{nf}$ ) and the input matching network ( $Q_{in}$ ), the NF and input return loss ( $S_{11}$ ) frequency response of an LNA are controlled. According to different purposes such as narrowband or wideband LNAs, the Q-factors should be chosen properly. Medium- $Q_{nf}$  and high- $Q_{nf}$  cascode LNAs in CMOS technologies has been implemented for verifying validity of the proposed theory.

**Index Terms-** Noise figure, input matching, CMOS, low-noise amplifier, quality factor.

### I. INTRODUCTION

RF receiver front-ends, such as dual-band tri-mode receiver front-ends compliant with the IEEE 802.11a, b, and g standards [1], or even much higher frequency 60-GHz receiver front-ends [2], have drawn lots of attention. This is mainly attributed to the rapid evolution of the relatively low-cost CMOS technology and the fast development of wireless communication techniques. Low-noise amplifiers (LNAs), which amplify the small radio-signals received from the antenna with a good signal-to-noise ratio property over the whole band of interest, is a critical block in receiver front-end design. The general requirements of an LNA include high and flat power gain  $S_{21}$ , good input impedance matching (i.e. low input return loss  $S_{11}$ ), and low and flat noise figure (NF) performances across the whole band of interest.

For a narrow-band LNA, the methodology to find the optimum NF at a specific center frequency under the power-dissipation constraint has been proposed [3]. However, by using this approach, only a single frequency is considered in the NF curve. Thus, an unacceptable sharp NF curve may be resulted in [4]. For example, the 2-9 GHz CMOS ultra-wideband (UWB) LNA in [5] exhibits simultaneous wideband  $S_{21}$  and  $S_{11}$  performance; however, the flatness of the measured NF of 2.5-7.4 dB is not satisfactory. Besides, the 3.1-10.6 GHz CMOS UWB LNA in [6] also exhibits simultaneous wideband  $S_{21}$  and  $S_{11}$  performance, but the flatness of the measured NF of 4-9.3 dB is again not satisfactory.

In this work, a method for optimizing a low-noise amplifier (LNA) with understanding Frequency responses of its noise figure (NF) and input matching

characteristics is introduced. The method involves the determination of the quality factor (Q-factor) of the NF ( $Q_{nf}$ ) and the Q-factor of the input matching network ( $Q_{in}$ ). It is found that the NF and the  $S_{11}$  frequency responses of an LNA can be controlled by  $Q_{nf}$  and  $Q_{in}$ , respectively. Since the value of  $Q_{nf}$  is proportional to that of  $Q_{in}$ , there is a compromise between input matching bandwidth and low NF. The NF and the  $S_{11}$  frequency responses of a cascode LNA with inductive source degeneration are derived in Section II. To verify the proposed theory, a medium- $Q_{nf}$  LNA and a high- $Q_{nf}$  LNA both with center frequency of 5.5 GHz were designed in section III. The experimental results of the medium  $Q_{nf}$  LNA and the high  $Q_{nf}$  LNA are discussed in Section IV. Section V is the conclusion.

### II. FREQUENCY RESPONSES OF A LNA

#### A. NF Frequency Response

A famous cascode LNA with inductive source degeneration shown in Fig. 1(a). Fig. 1(b) is input noise equivalent circuit of Fig. 1(a). where  $e_s$ ,  $e_{lg}$ ,  $e_{rg}$ ,  $e_{ls}$ , and  $e_{rs}$  represent the thermal noise voltages of the source resistance  $R_s$ , series resistance  $R_{Lg1}$  of gate inductor  $L_{G1}$ , transistor gate resistance  $R_{g1}$ , series resistance  $R_{Ls1}$  of source inductor  $L_{S1}$ , and transistor source resistance  $R_{s1}$ ;  $i_g$  and  $i_d$  represent the gate induced and channel resistance thermal noise currents. Now the noise factor F of the LNA ( $NF=10 \cdot \log_{10} F$ ) can be expressed as follows [7]:

$$F = 1 + \frac{R_{par}}{R_s} + F_{gn} + F_{dn} \quad (1)$$

Where  $F_{gn} (= \frac{|i_{go}|^2}{|i_{so}|^2})$  and  $F_{dn} (= \frac{|i_{do}|^2}{|i_{so}|^2})$  represent the corresponding noise factor contributions of  $i_{go}$  and  $i_{do}$  to the LNA, respectively.  $\delta$  and  $\gamma$  are the coefficients

of gate noise and channel noise. Based on the measured results in [8],  $\delta$  of 4.1 and  $\gamma$  of 2.21 are adopted for the following NF calculation.  $i_{n,out}$  stands for the total noise current in the short-circuited output path originated from the noise

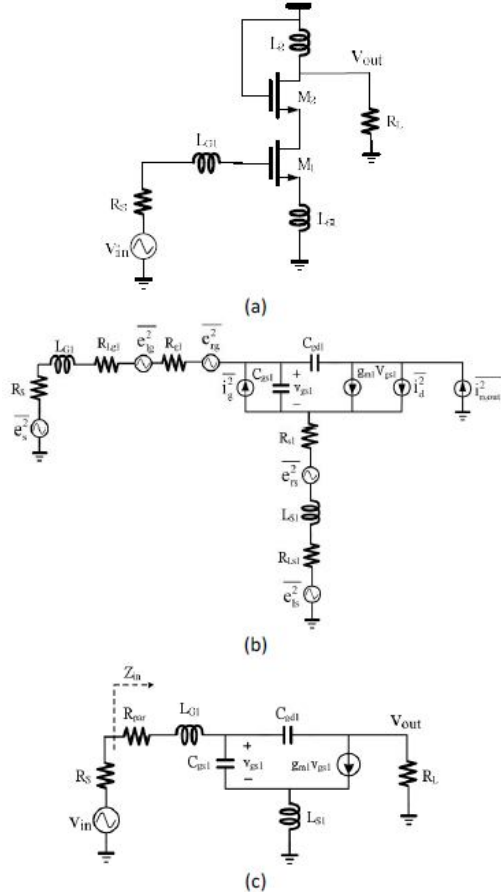


Fig. 1 (a) Schematic of the cascode LNA with inductive source degeneration. (Biasing not shown.) (b) Input noise equivalent circuit of Fig. 1(a). (c) Input small-signal equivalent circuit of Fig. 1(a).

current components  $i_{s0}$ ,  $i_{g0}$ ,  $i_{r0}$ ,  $i_{rs0}$ ,  $i_{l0}$ ,  $i_{g0}$ , and  $i_{d0}$  produced by the noise generators from  $e_s$ ,  $e_g$ ,  $e_r$ ,  $e_{rs}$ ,  $e_{ls}$ ,  $i_g$ , and  $i_d$ , respectively.  $R_{par} (=R_{l_{g1}} + R_{g1} + R_{l_{s1}} + R_{s1})$  is the total series parasitic resistance. Note that  $R_{par}$  is part of the input resistance  $R_{in} (=R_{par} + \omega_{T1}L_{S1})$ , where  $\omega_{T1} = g_{m1}/C_{gs1}$  is the current-gain cut-off frequency of  $M_1$ , which is usually close to 50 W over the band of interest. The noise factor  $F$  of the LNA can be shown as follows:

$$F = 1 + \frac{R_{par}}{R_s} + \frac{\delta \alpha \omega^2 C_{gs1}^2 R_s}{5g_{m1}} + \frac{\gamma}{\alpha R_s g_{m1}} \cdot \left[ \left( \frac{s}{\omega_{nf}} \right)^2 + \frac{s}{\omega_{nf} Q_{nf}} + 1 \right]^2 \quad (2)$$

in which

$$\omega_{nf} = \frac{1}{\sqrt{(L_{G1} + L_{S1}) \cdot (C_{gs1} + C_{gd1})}} \quad (3)$$

and

$$Q_{nf} = \frac{1}{R_s + R_{par}} \cdot \sqrt{\frac{L_{G1} + L_{S1}}{C_{gs1} + C_{gd1}}} \quad (4)$$

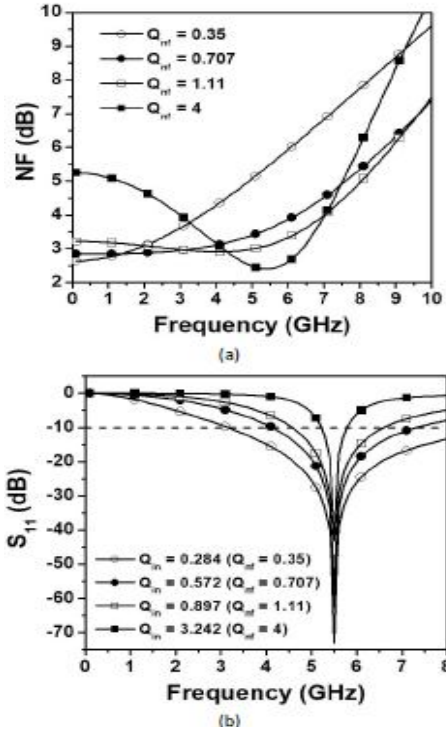


Fig. 2 Calculated (a) NF, and (b)  $S_{11}$  versus frequency characteristics for the LNA with  $Q_{nf}$  as a variable.

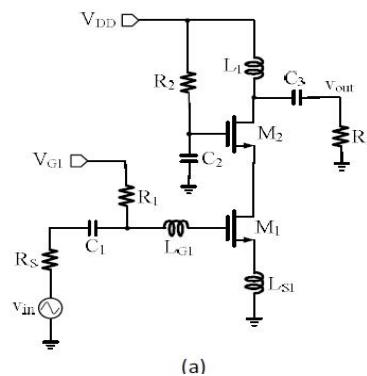
Where  $\omega_{nf}$  and  $Q_{nf}$  present the resonance frequency and the Q-factor of the input noise equivalent circuit. To gain more insight, we can disregard the effect of the third term in (2) temporarily. Since the frequency response of the NF has the form of a second-order function of  $s$ , which is controlled by  $Q_{nf}$ . That is, a narrowband or wideband NF frequency response can be achieved by adopting a relatively larger or smaller  $Q_{nf}$ , which will be explained in more detail later.

### B. $S_{11}$ Frequency Response

Fig. 1(d) shows the input small-signal equivalent circuit of Fig. 1(a), where  $R_L$  represents the output resistive load of  $M_1$ . Therefore, the  $S_{11}$  of the LNA in Fig. 1(a) can be expressed as follows:

$$S_{11} = \frac{s^2 + \omega_m^2}{s^2 + s \frac{\omega_m}{Q_{in}} + \omega_m^2} \quad (5)$$

in which



(a)

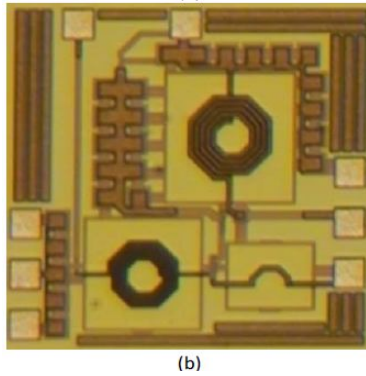


Fig. 3 (a) Schematic, and (b) chip micrograph of the cascode LNA with a medium  $Q_{nf}$  of 1.3.

$$\omega_{in} = \frac{1}{\sqrt{(L_{G1} + L_{S1})[C_{gs1} + C_{gd1}(1 + g_{m1}R_L)]}} \quad (6)$$

and

$$Q_{in} = \frac{1}{2R_s} \cdot \sqrt{\frac{L_{G1} + L_{S1}}{[C_{gs1} + C_{gd1}(1 + g_{m1}R_L)]}} \quad (7)$$

$\omega_{in}$  and  $Q_{in}$  present the resonant frequency and the Q-factor of the input small-signal equivalent circuit [9].  $|S_{11}|$  is a standard notch function. Its  $-10$  dB bandwidth  $\Delta f_{10dB}$ , i.e. the bandwidth corresponding to  $20 \log |S_{11}| \leq -10$  dB, can be expressed as follows [10]:

$$\Delta f_{10dB} \approx \frac{100}{6\pi(L_{G1} + L_{S1})} \quad (8)$$

That is, the input matching bandwidth  $\Delta f_{10dB}$  is inversely proportional to the value of  $L_{G1} + L_{S1}$ .

It is interesting to note that  $\omega_{nf}$  (see (3)) is equal to  $\omega_{in}$  (see (6)) of the input network except that the coefficient of the capacitance term  $C_{gd1}$  is smaller.  $Q_{nf}$  (see (4)) is equal to  $Q_{in}$  (see (7)) of the input network except that the resistance term  $\omega_{T1}L_{S1}$  is excluded, and the coefficient of the capacitance term  $C_{gd1}$  is smaller. Note that  $\omega_{T1}L_{S1}$  is an equivalent resistance originated from the series-series

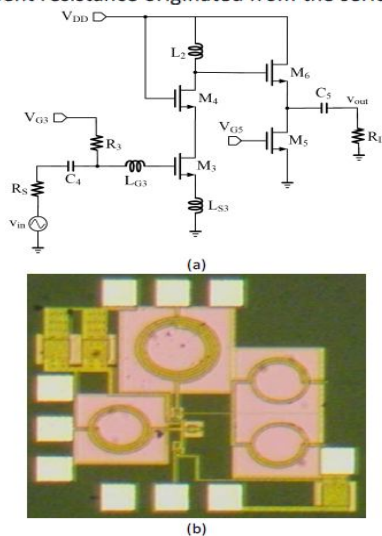
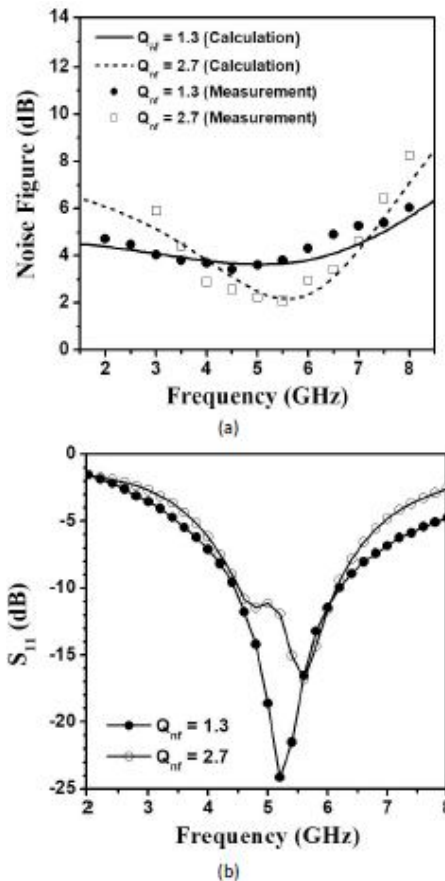


Fig. 4 (a) Schematic, and (b) chip micrograph of the cascode LNA with a high  $Q_{nf}$  of 2.7.

feedback inductor  $L_{S1}$ . So it is reasonable that  $\omega_{T1}L_{S1}$  is excluded in the resistance term of  $Q_{nf}$  since it is not a real resistance.

Fig. 2(a) shows the characteristics of calculated NF versus frequency of the cascode LNA with  $Q_{nf}$  as a variable. As can be seen, in the case of a low  $Q_{nf}$  (such as 0.35), NF increases rapidly with the increase of frequency, not suitable for wideband LNAs. This is because in the case of a low  $Q_{nf}$ , the quadratic function in (2) is dominated by the first-order term  $j\omega/(\omega_{nf}Q_{nf})$ . This explains why some wideband LNAs [5], [6], [11], [12] in the literature exhibited flat gain, but the corresponding NF response increased rapidly with the increase of frequency. In the case of a medium  $Q_{nf}$  (such as 0.707 or 1.11), the flat NF responses suitable for wideband LNAs was achieved. Furthermore, in the case of a relatively higher  $Q_{nf}$  (such as 4), the corresponding NF curve shows a sharp shape with a deep valley at frequency of 5.5 GHz. That is, a narrowband low and flat NF frequency response can be achieved. This is because in the case of a high  $Q_{nf}$ , the first-order term  $j\omega/(\omega_{nf}Q_{nf})$  in the quadratic function of (2) becomes relatively negligible. The literature [4] is an example of the narrowband NF response with high  $Q_{nf}$ . Fig. 2(b) shows the calculated  $S_{11}$  versus frequency characteristics of the cascode LNA with  $Q_{in}$  (or  $Q_{nf}$ ) as a variable. As can be seen,



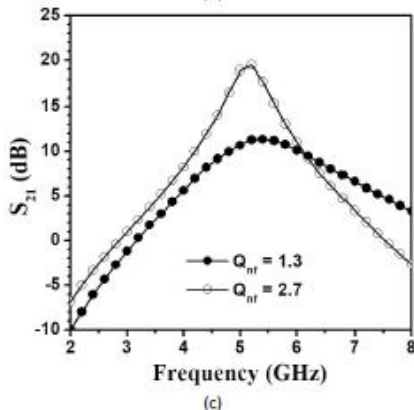


Fig. 5 Measured (a) NF, (b)  $S_{11}$ , and (c)  $S_{21}$  versus frequency characteristics of the medium- $Q_{nf}$  LNA and the high- $Q_{nf}$  LNA.

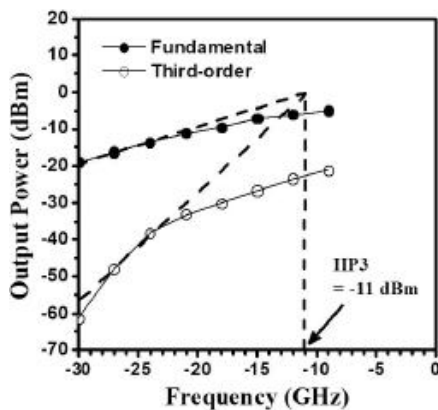


Fig. 6 Measured IIP<sub>3</sub> of the medium- $Q_{nf}$  LNA.

$\Delta f_{10dB}$  is indeed inversely proportional to the value of  $L_{G1}+L_{S1}$  (or  $Q_{in}$ ). That is, there is a compromise between input matching bandwidth and low NF.  $Q_{in}$  or  $Q_{nf}$  should be chosen for realizing narrowband or wideband LNAs. A narrowband NF frequency response can be achieved by adopting a relatively larger  $Q_{nf}$ , which is an under-damped response. On the other hand, a wideband NF frequency response can be

achieved by adopting a relatively smaller  $Q_{nf}$ , which is an under-damped response.

### III. LNA CIRCUIT DESIGN WITH DIFFERENT Q-FACTORS

To verify the effect of  $Q_{nf}$  on the NF and input matching frequency responses of LNAs, a medium  $Q_{nf}$  (1.3) LNA and a high  $Q_{nf}$  (2.7) LNA both with center frequency ( $f_{in}$ ) of 5.5 GHz were implemented by 0.18  $\mu\text{m}$  and 0.25  $\mu\text{m}$  CMOS technologies, respectively. These LNAs has similar first cascode stages with different transistor sizes for realizing narrowband and wideband NF and input matching frequency responses.

#### A. Medium- $Q_{nf}$ LNA Circuit Design

Fig. 3(a) shows the schematic of the LNA with a medium (or relatively lower)  $Q_{nf}$  of 1.3. This LNA was designed for achieving a relatively wider NF and input matching bandwidth with center frequency of 5.5 GHz. Basically, this CMOS LNA was a cascode amplifier ( $M_1$  and  $M_2$ ) with one source-degenerative inductor ( $L_{S1}$ ) and one gate inductor ( $L_{G1}$ ) for simultaneous input-impedance and noise matching.  $L_1$  and  $C_3$  function as the tuned load. According to (3) and (4), a relatively smaller  $L_{G1}+L_{S1}$  and larger  $C_{gs1}+C_{gd1}$  should be chosen for a medium- $Q_{nf}$  LNA. Hence, a relatively larger size of 250  $\mu\text{m}/0.18 \mu\text{m}$  was selected for  $M_1$  to obtain a relatively larger  $C_{gs1}$  of 176 fF and  $C_{gd1}$  of 72 fF. In addition, relatively smaller inductance of 2.54 nH and 0.2 nH was chosen for inductors  $L_{G1}$  and  $L_{S1}$ , respectively. The other component parameters were as follows:  $C_1 = 4.76$  pF,  $C_2 = 9.52$  pF,  $C_3 = 186$  fF,  $L_1 = 2.55$  nH,  $R_1 = 3$  k $\Omega$ , and  $R_2 = 3$  k $\Omega$ . The size of 125  $\mu\text{m}/0.18 \mu\text{m}$  was selected

	NF (dB)	NF Variation (dB)	Gain (dB)	$S_{11}$ Bandwidth (GHz)	IIP <sub>3</sub> (dBm)	Power Consumption (mW)
This Work (Medium $Q_{nf} = 1.3$ )	3.4 ~ 6 (2 ~ 8 GHz)	2.6	11.3	1.78 (4.41 ~ 6.19 GHz)	-11	12.6
This Work (High $Q_{nf} = 2.7$ )	2.1 ~ 8.3 (3 ~ 8 GHz)	6.2	19.5	1.64 (4.51 ~ 6.15 GHz)	N/A	17.8
[5] 2 ~ 9 GHz LNA	2.5 ~ 7.4 (2 ~ 9 GHz)	4.9	13.5	7 (2 ~ 9 GHz)	-5.4	25.2
[6] 3.1 ~ 10.6 GHz LNA	4 ~ 9.3 (3.1 ~ 10.6 GHz)	5.3	9.3	9.1 (2.6 ~ 11.7 GHz)	-6.7	9
[14] 2.6 ~ 10.2 GHz LNA	3 ~ 7 (3 ~ 5 GHz)	4	12.5	7 (3.5 ~ 10.5 GHz)	-7	7.2

Table I Summary of the implemented medium- $Q_{nf}$  LNA, high- $Q_{nf}$  LNA, and the CMOS UWB LNAs.

for  $M_2$ . Fig. 3(b) shows the chip micrograph of the LNA with  $Q_{nf}$  of 1.3. The chip area was only 0.4 mm<sup>2</sup> excluding the testing pads.

#### B. High- $Q_{nf}$ LNA Circuit Design

Fig. 4(a) shows the schematic of the LNA with a high (or relatively higher)  $Q_{nf}$  of 2.7. This LNA is designed

in order to achieve a relatively narrower and lower NF over the narrower frequency band of interest. The center frequency is also 5.5 GHz. This LNA is basically a cascode amplifier ( $M_3$  and  $M_4$ ) with one

source-degenerative inductor ( $L_{S3}$ ) and one gate inductor ( $L_{G3}$ ) for simultaneous input impedance and noise-matching.  $L_2$  and  $C_{d4}$  (the total parasitic capacitance at the drain of transistor  $M_4$ ) function as the tuned load of the cascode amplifier. The major difference is that a source follower composed of  $M_6$  and a current source ( $M_5$ ) was added to be a buffer for test purposes [13]. According to (3) and (4), a relatively larger  $L_{G3}+L_{S3}$  and smaller  $C_{gs3}+C_{gd3}$  should be chosen for a high- $Q_{nf}$  LNA. Hence, a relatively smaller gate size of 110  $\mu\text{m}/0.24$   $\mu\text{m}$  was selected for  $M_3$  to obtain a relatively smaller  $C_{gs3}$  of 135 fF and  $C_{gd3}$  of 49 fF. In addition, relatively larger inductance of 3.8 nH and 0.26 nH was chosen for inductors  $L_{G3}$  and  $L_{S3}$ , respectively. The inductance of  $L_2$  was 1.5 nH. The sizes of  $M_4$ ,  $M_5$ , and  $M_6$  are 1210  $\mu\text{m}/0.24$   $\mu\text{m}$ , 1210  $\mu\text{m}/0.24$   $\mu\text{m}$ , 810  $\mu\text{m}/0.24$   $\mu\text{m}$ , respectively. Fig. 4(b) shows the chip micrograph of the LNA with  $Q_{nf}$  of 2.7. The chip area was only 0.28  $\text{mm}^2$  excluding the testing pads.

#### IV. MEASUREMENT RESULTS AND DISCUSSIONS

The noise and scattering parameters were measured on-wafer. For the CMOS LNA with a medium  $Q_{nf}$  of 1.3, the LNA drained 7 mA current from a supply voltage ( $V_{DD}$ ) of 1.8 V, i.e. it consumed only 12.6 mW power. For the CMOS LNA with a high  $Q_{nf}$  of 2.7, the LNA drained 7.1 mA current from a  $V_{DD}$  of 2.5 V, i.e. it consumed 17.8 mW power. Fig. 5(a) shows the measured and calculated NF versus frequency characteristics of the medium  $Q_{nf}$  LNA and the high  $Q_{nf}$  LNA. For the medium  $Q_{nf}$  LNA, flat NF of 3.4-6 dB (or  $4.7\pm 1.3$  dB) was achieved over the frequency range of 2-8 GHz. Besides, for the high  $Q_{nf}$  LNA, its NF curve shows a sharp deep valley, i.e. an under-damped response. The corresponding NF was 2.1-8.3 dB (or  $5.2\pm 3.1$  dB) over the frequency range of 3-8 GHz. The result is consistent with the theory in Section II.

Fig. 5(b) shows the measured  $S_{11}$  versus frequency characteristics of the medium- $Q_{nf}$  LNA and the high  $Q_{nf}$  LNA. The measured  $S_{11}$  of the medium- $Q_{nf}$  LNA was below -10 dB from 4.41 GHz to 6.19 GHz, i.e. the input matching bandwidth was 1.78 GHz. Besides, the measured  $S_{11}$  of the high- $Q_{nf}$  LNA was below -10 dB from 4.51 GHz to 6.15 GHz, i.e. the input matching bandwidth was 1.64 GHz. The trend of the measurement results is consistent with the theory in Section II.

Fig. 5(c) shows the measured  $S_{21}$  versus frequency characteristics of the medium- $Q_{nf}$  LNA and the high  $Q_{nf}$  LNA. The peak  $S_{21}$  of the high- $Q_{nf}$  LNA was 19.5 dB (at 5.2 GHz), which is 8.2 dB higher than that (11.3 dB at 5.4 GHz) of the medium  $Q_{nf}$  LNA. The reason why the high  $Q_{nf}$  LNA exhibited higher  $S_{21}$  is mainly

due to the addition of the buffer stage. The cost is a higher power-consumption (17.8 mW v.s. 12.6 mW). Fig. 6 shows the measured input three-order inter-modulation point ( $IIP_3$ ) of the medium- $Q_{nf}$  LNA is -11 dBm.

Table I is a summary of the implemented medium- $Q_{nf}$  LNA, high- $Q_{nf}$  LNA, and the CMOS UWB LNAs. As can be seen, compared with the high- $Q_{nf}$  LNA, the medium- $Q_{nf}$  LNA exhibited wider input matching bandwidth and flatter NF frequency response due to smaller  $Q_{in}$  and  $Q_{nf}$ , respectively. Besides, due to the selected medium  $Q_{nf}$  of 1.3, the medium- $Q_{nf}$  LNA achieved a flatter NF frequency response (NF variation was only 2.6 dB over 2-8 GHz) than the 2-9 GHz CMOS UWB LNA (NF variation was 4.9 dB) in [5], the 3.1-10.6 GHz UWB LNA (NF variation was 5.3 dB) in [6], and the 2.6-10.2 GHz CMOS UWB LNA (NF variation was 4 dB) in [14].

#### CONCLUSION

In this paper, we introduce the methodology of hand analysis to estimate the NF and  $S_{11}$  frequency responses of an LNA. The NF and  $S_{11}$  frequency responses of an LNA can be controlled by  $Q_{nf}$  and  $Q_{in}$ , respectively. A medium  $Q_{nf}$  (1.3) LNA and a high  $Q_{nf}$  (2.7) LNA with center frequency of 5.5 GHz fabricated with 0.18  $\mu\text{m}$  and 0.25  $\mu\text{m}$  CMOS processes, respectively, were used to verify the proposed theory. The measurement results show that medium  $Q_{nf}$  frequency response is suitable for wideband application, while high  $Q_{nf}$  frequency response is suitable for narrowband application.

#### ACKNOWLEDGEMENT

This work was supported in part by the Ministry of Science and Technology of Taiwan under Contract MOST 105-2622-8-002-002. The authors are very grateful for the support from the National Chip Implementation Center (CIC) for chip fabrication, and National Nano-Device Laboratory (NDL) for high-frequency measurements.

#### REFERENCES

- [1] K. R. Rao, J. Wilson, and M. Ismail, "A CMOS RF front-end for a multistandard WLAN receiver," *IEEE Microwave and Wireless Components Letters*, vol. 15, no. 5, pp. 321-323, May 2005.
- [2] B. Razavi, "A 60-GHz CMOS receiver front-end," *IEEE J. Solid-State Circuits*, vol. 41, no. 1, pp. 17-22, Jan. 2006.
- [3] D. K. Shaeffer, and T. H. Lee, "A 1.5V, 1.5GHz CMOS Low Noise Amplifier," *IEEE J. Solid-State Circuits*, vol. 32, no. 5, pp. 745-759, May 1997.
- [4] D. J. Cassan, and J. R. Long, "A 1-V transformer-feedback low-noise amplifier for 5-GHz wireless LAN in 0.18- $\mu\text{m}$  CMOS," *IEEE J. Solid-State Circuits*, vol. 38, no. 3, pp. 427-435, Mar. 2003.

- [5] C. W. Kim, M. S. Jung, and S. G. Lee, "Ultra-wideband CMOS Low Noise Amplifier," *Electronics Letters*, vol. 41, no. 7, pp. 384-385, Mar. 2005.
- [6] A. Bevilacqua and A. M. Niknejad, "An Ultrawideband CMOS Low-Noise Amplifier for 3.1- 10.6-GHz Wireless Receivers," *IEEE J. Solid-State Circuits*, vol. 39, pp. 2259-2268, Dec. 2004.
- [7] H. W. Chiu, S. S. Lu, and Y. S. Lin, "A 2.17 dB NF, 5 GHz Band Monolithic CMOS LNA with 10 mW DC Power Consumption," *IEEE Trans. Microwave Theory and Technique*, vol. 53, no. 3, pp. 813-824, Mar. 2005.
- [8] P. Heydari, "Design and Analysis of Performance-Optimized CMOS UWB Distributed LNA," *IEEE J. Solid-State Circuits*, vol. 42, no. 9, pp. 1892-1905, Sep. 2007.
- [9] A. S. Sedra, and K. C. Smith, *Microelectronic Circuits*, 5th ed., Oxford University Press, New York, USA, 2004, pp. 840, and 1103-1105.
- [10] T. Wang, H. C. Chen, H. W. Chiu, Y. S. Lin, G. W. Huang, and S. S. Lu "Micromachined CMOS LNA and VCO By CMOS Compatible ICP Deep Trench Technology," *IEEE Tran. on Microwave Theory and Technique*, vol. 54, no. 2, Feb. 2006.
- [11] K. H. Chen, J. H. Lu, B. J. Chen and S. I. Liu, "An Ultra-Wide-Band 0.4-10-GHz LNA in 0.18  $\mu\text{m}$  CMOS," *IEEE Trans. Circuits and Systems-II*, vol. 54, pp. 217-221, Mar. 2007.
- [12] Q. Li and Y. P. Zhang, "A 1.5 V 2-9.6 GHz Inductorless Low-Noise Amplifier in 0.13  $\mu\text{m}$  CMOS," *IEEE Trans. Microwave Theory and Techniques*, vol.55, no.10, pp. 2015-2023, Oct. 2007.
- [13] C. W. Kim, M. S. Kang, P. T. Anh, H. T. Kim, and S. G. Lee, "An Ultra-Wideband CMOS Low Noise Amplifier for 3-5-GHz UWB System," *IEEE J. of Solid-State Circuits*, vol. 40, no. 2, pp. 544-547, Feb. 2005.
- [14] G. Sapone and G. Palmisano, "A 3–10-GHz low-power CMOS low-noise amplifier for ultra-wideband communication," *IEEE Trans. Microw. Theory Techn.*, vol. 59, no. 3, pp. 678–686, Mar. 2011.

★ ★ ★